

SINGLE BUNCH COLLECTIVE EFFECTS IN THE EBS STORAGE RING

L. R. Carver, E. Buratin, N. Carmignani, F. Ewald, L. Hoummi,
S. Liuzzo, T. Perron, B. Roche, S. White
European Synchrotron Radiation Facility, Grenoble, France

Abstract

The ESRF storage ring (SR) has been dismantled and replaced by the Extremely Brilliant Source (EBS) which has now been commissioned. Beam based measurements have been performed to characterise the impedance of the new machine and to make a first comparison with predictions. The results from instability threshold scans and tune shift measurements will be presented, as well as bunch length and position variation with current and microwave threshold measurements.

INTRODUCTION

The ESRF-EBS is a new 4th generation light source located at the European Synchrotron Radiation Facility and was commissioned starting in 2019 and has been in user operation since 2020 [1]. The EBS is currently producing light with brilliance and coherence that are orders of magnitudes better than its predecessor [2].

When operating with high beam currents, limitations will arise coming from the beams interaction with the vacuum chamber. These limitations may require a transverse feedback, or higher chromaticities to mitigate them, which could result in lower beam lifetimes [3]. In order to better understand the current machine performance and predict the performance of future running scenarios (higher single bunch currents, smaller in-vacuum undulator (IVU) gaps), an accurate impedance model is needed. Single bunch measurements of both the longitudinal and transverse impedances have started and are beginning to shine light on the accuracy of the impedance model. Future iterations on the impedance model hope to rectify any observed discrepancies.

This report will first briefly describe the development of the impedance model and how the single bunch predictions are made. Then the single bunch measurements will be described and compared to predictions.

EBS IMPEDANCE MODEL

The EBS machine has several different types of vacuum chambers. All chambers have horizontal apertures of ± 25 mm (in reality the antechamber is much larger than this but the impedance contribution is minor). Vertical apertures are either ± 10 mm (large) or ± 6.5 mm (small). Chambers are made of either stainless steel or aluminium. Special chambers for the insertion devices (IDs) and the kickers are also present. An example of a vacuum chamber profile is shown in Fig. 1. The aperture/material combinations were simulated in CST (or IW2D for the more special chambers) using the full omega profile of the chamber and weighted appropriately by length and beta function.

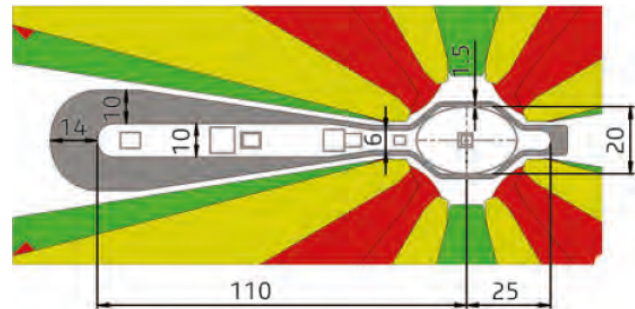


Figure 1: The vacuum chamber profile. The beam passes through the chamber on the right hand side, while the ante chamber on the left is for the synchrotron radiation. For the impedance modelling, only the profile close to the beam is considered.

The geometric impedance was simulated in GdfidL using a longitudinal gaussian profile with a sigma of 1 mm [4]. The geometric impedance is comprised of those chambers with geometric changes, (e.g. tapers) or discontinuities (e.g. collimators).

To perform simulations of the single bunch collective effects, PyAT (Python Accelerator Toolbox) was used [5]. Developments in PyAT have recently been made to include the *fast ring* function, which can reduce a full accelerator lattice into a handful of transfer matrices: linear 6x6 tracking, non-linear effects (including amplitude detuning), and a quantum diffusion element to maintain the correct equilibrium emittances in the 3 planes. This greatly speeds up the computation and can allow a large number of macroparticles to be simulated. A lumped impedance element was included in the lattice which performs the standard slicing and wake propagation through the slices. For simulations in the longitudinal plane, only the longitudinal impedance was simulated. For the transverse plane, all of the impedances (longitudinal, dipolar and quadrupolar) were included to ensure any bunch lengthening effects were taken into account. Typically when comparing simulations to measurements, identical parameters were taken (i.e. the same currents) and the post processing of both measurements and simulations were very similar.

In this report, the simulations are only provided for the case where the IVU gaps are open. Additional simulations are required to further model the geometric impedance of the IVU tanks when they are closed. The gaps open case is an easily reproducible case but also more pessimistic due to the much larger taper angle.

LONGITUDINAL IMPEDANCE MEASUREMENTS

The longitudinal impedance can be characterised with three distinct measurements, firstly the bunch length variation with current shown in Eq. (1),

$$\frac{\sigma_t}{\sigma_{t0}} - \frac{\sigma_t}{\sigma_{t0}} = \frac{I_b \alpha}{\sqrt{2\pi} \nu_s^2 \omega_0^3 \sigma_{t0}^3 E/e} \text{Im} \left(\frac{Z_{\parallel}}{n} \right)_{\text{eff}}, \quad (1)$$

where σ_t is the bunch length, σ_{t0} is the zero current bunch length, I_b is the bunch current, α is the momentum compaction factor, ω_0 is the revolution frequency, ν_s is the synchrotron tune, E is the beam energy, e is the elementary charge, and Z_{\parallel}/n is the normalised longitudinal impedance. Secondly the bunch position shift (which is a measure of the energy loss due to impedance) with current. This is directly related to the loss parameter which is shown in Eq. (2) [6]

$$k_n(\sigma_t) = \frac{\omega_0}{\pi} \sum_{p=0}^{\infty} \text{Re} Z_n(p\omega_0) \exp[-(p\omega_0\sigma_t)^2]. \quad (2)$$

Finally the microwave threshold (MWT) which is often approximated by the Boussard criterion [7].

Both the bunch length and the loss factors are dominated by the low frequency part of the broadband impedance whereas the MWT is also sensitive to high frequency resonators and requires more detailed analytical descriptions (involving Vlasovs theory [3]).

The bunch profiles and the bunch phase shift were measured with a dual time base streak camera (Hamamatsu C10910 [8]) installed in the visible light diagnostics beamline of the ESRF (for a general overview on streak cameras used in synchrotrons see [9]). The visible light originates from the two permanent magnet dipoles. It contains radiation contributions from their nominal field strength (0.6 T) and their fringe fields. The light is extracted from the storage ring via a cooled aluminium half mirror, through a UV UHV-window and steered into a dedicated hutch in the experimental hall.

The results of each of these three measurements can be found in Figs. 2, 3 and 4. It can be seen that the broadband real and imaginary impedances are in good agreement with the model as shown by the bunch length variation and the weighted center versus current. The MWT was measured to be almost a factor 3 lower than predicted. This means that the discrepancy likely arises from the high frequency part of the impedance. Studies are underway to explore possible sources of this difference.

TRANSVERSE IMPEDANCE MEASUREMENTS

It is clear that the source of the discrepancy in the MWT will also have an impact on the transverse impedance too, therefore some differences can be expected.

Table 1 shows a summary of the predicted and the measured threshold for the Transverse Mode Coupling Instability

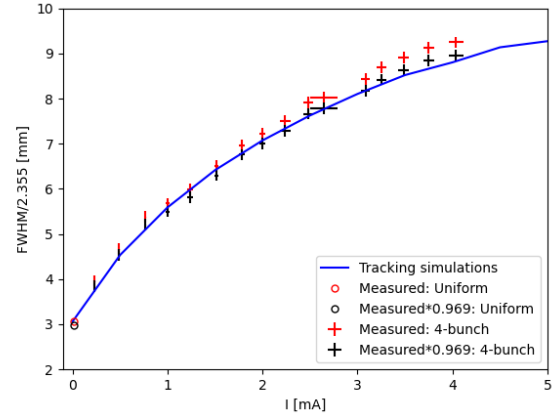


Figure 2: The measured bunch length versus single bunch current compared with simulations. No difference was measured between gaps open or gaps closed.

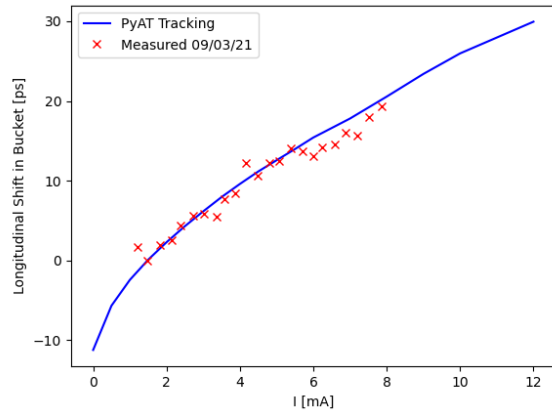


Figure 3: Longitudinal shift of the bunch versus current, compared to simulations. The noise of the data will be reduced in the future with new settings for the streak camera.

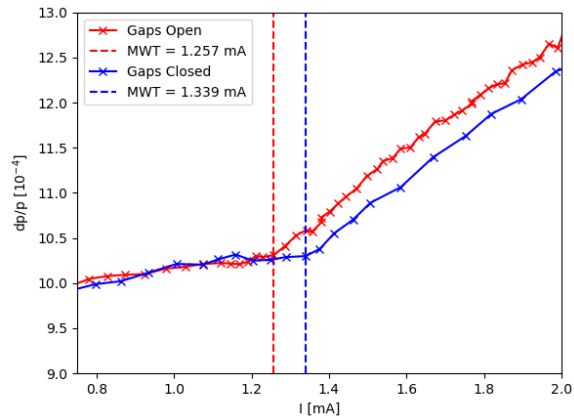


Figure 4: Measured MWTs for IVU open and closed. The simulated threshold is not shown but was calculated as 3.5 mA. Gaps open threshold is lower due to the large taper angle of the IVU tanks.

(TMCI) and the rate at which the tune (mode 0 of the bunch) is linearly shifting below this threshold. The measured TMCI threshold is about 20% lower than predicted, indicating the transverse impedance model is underestimated. In the simulations, the dipole and quadrupole wake potentials have opposite signs which are largely cancelling each other out. In the vertical plane the wakes have the same sign, increasing the measured tune shift. This is the general case for flat chambers [10]. The measured tune shifts reflect this and are larger in V than in H, however the measured shifts are both larger than predicted.

Table 1: Measured Mode 0 Tune Shifts and TMCI Thresholds for $Q'=0$, the Error on the Tune Shifts Is Estimated From the Width of the Spectrum Which Was Deformed During the Measurements

	Simulated	Measured	Units
TMCI	0.53	0.44	mA
Tune Shift V	-4.988	-6.712 ± 2.402	10^{-3} /mA
Tune Shift H	-0.501	-1.082 ± 2.402	10^{-3} /mA

Figure 5 shows the measured and simulated mode shifts for $Q' = 1.5$. The shift of the modes that were measured can be well reproduced in the simulations, highlighting that the impedance model captures all of the key features needed to reproduce the beam behaviour.

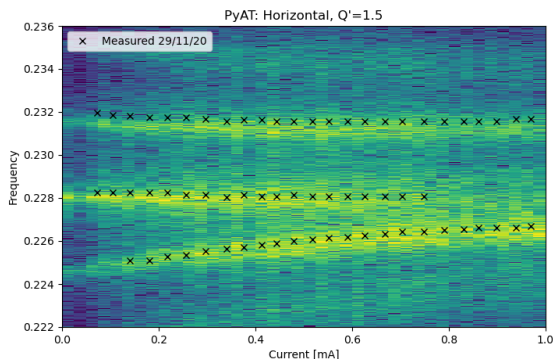


Figure 5: Horizontal mode shift at $Q'=1.5$. The black crosses are peaks coming from the measured spectrum, whereas the colored background is the simulated spectrum.

The current threshold as a function of chromaticity has also been measured and compared with simulations for the vertical plane only. The results of this scan are shown in Fig. 6. During the measurements, the chromaticity was moved along the diagonal ($Q'_x = Q'_y$), and for each step the current was increased until the beam became unstable in the vertical plane. After this, the vertical transverse feedback was switched on to stabilise the beam and the current could be increased further to allow a measurement of the horizontal threshold. At present, simulations for the horizontal plane have not yet been made as further characterisation on

the performance of the feedback is needed. Here, only the vertical plane is shown.

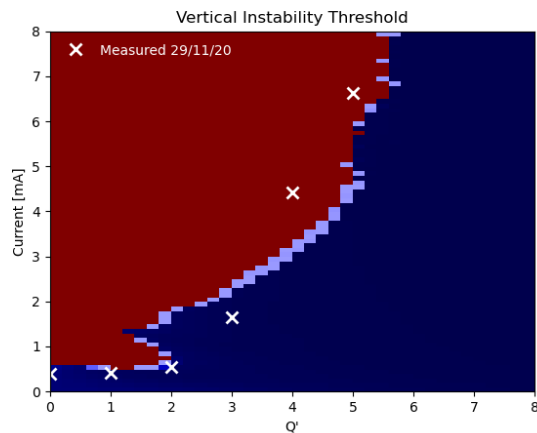


Figure 6: Vertical instability threshold as a function of chromaticity. The white crosses are measurements, the shaded regions show the area of stability (blue) or instability (red).

In general, good agreement for the studied chromaticity range is seen when comparing the measured and the simulated thresholds. For chromaticities above 6, we were not able to reach the threshold when making the measurement, as there are limitations due to heating of the ceramic kickers at high single bunch current. At Q' between 1 and 2, it is possible to see mode decoupling, creating a stable ‘horn-shaped’ region. Further measurements are planned to try and investigate this further.

CONCLUSIONS & FUTURE PLANS

As a first iteration on the impedance model, very good agreement is found in almost all aspects of the measurements, except for the MWT. This discrepancy is currently under investigation with possible sources already identified. Future iterations on the impedance model will also include a revised IVU model, a model of the collimators and striplines that include pumping ports and some special BPMs.

The measurements of the bunch position will be redone to improve the signal quality from the camera, and also needs to be repeated for gaps closed. This is planned for the near future.

Validation of the resistive wall impedance with multi-bunch measurements has already started, with some preliminary intensity threshold and grow damp measurements being taken. Simulations of uniform filling multi-bunch threshold will be performed in order to compare, while grow damp measurements will be fitted with an analytical formula.

REFERENCES

- [1] R. Dimper, H. Reichert, P. Raimondi, L. Ortiz, F. Sette, and J. Susini, “ESRF upgrade programme phase II”, ESRF, Grenoble, France, 2014.

- [2] L. Farvacque *et al.*, “A Low-Emittance Lattice for the ESRF”, in *Proc. 4th Int. Particle Accelerator Conf. (IPAC’13)*, Shanghai, China, May 2013, paper MOPEA008, pp. 79-81.
- [3] A. Chao, *Physics of Collective Beam Instabilities in High Energy Accelerators*, Dallas, Texas, USA: Wiley, 1993.
- [4] S. M. White, “Preliminary Longitudinal Impedance Model for the ESRF-EBS”, in *Proc. 8th Int. Particle Accelerator Conf. (IPAC’17)*, Copenhagen, Denmark, May 2017, pp. 3063-3066. doi:10.18429/JACoW-IPAC2017-WEPIK058
- [5] GitHub: Accelerator Toolbox Homepage, <https://github.com/atcollab>
- [6] B. W. Zotter and S.A. Kheifets, *Impedances and wakes in high-energy particle accelerators*, World Scientific, 2000.
- [7] D. Boussard, “Observation of longitudinal microwave instabilities in the CPS”, CERN, Geneva, Switzerland, CERN Report LabII/RF/Int./75-2, 1975.
- [8] Hamamatsu Universal Streak Camera, <https://www.hamamatsu.com/eu/en/product/type/C10910-05/index.html>
- [9] K. Scheidt, “Review of Streak Cameras for Accelerators: Features, Applications and Results”, in *Proc. 7th European Particle Accelerator Conf. (EPAC’00)*, Vienna, Austria, Jun. 2000, paper WEYF202, pp. 182-186.
- [10] N. Mounet, “The LHC Transverse Coupled Bunch Instability”, Ph.D. thesis, EPFL, Lausanne, Switzerland, 2012.